Journal of
Composites Science

MDPI

Brief Report

Replacement of Carbon Black with Coppiced Biochar in Guayule Rubber Composites Improves Tensile Properties

Steven C. Peterson [1,*] and Colleen M. McMahan [2]

[1] Plant Polymer Research, National Center for Agricultural Utilization Research, Agricultural Research Service, USDA, 1815 N. University Ave, Peoria, IL 61604, USA
[2] Bioproducts Research Unit, Western Regional Research Center, Agricultural Research Service, USDA, 800 Buchanan St., Albany, CA 94710, USA
* Correspondence: steve.peterson@usda.gov

Abstract: Natural rubber, sourced from *Hevea brasiliensis* trees mainly in southeast Asia, is a critically important resource for transportation, national security, and medical products, among other uses. The guayule shrub is a domestic alternative source of natural rubber that is emerging with advantages over Hevea since it is well-suited for many medical and consumer applications. Biochar is a sustainable form of carbon made from biomass that is a potential replacement for petroleum-sourced carbon black, the most common filler for rubber composites. The coppiced-wood species hybrid poplar (*Populus* × *canadensis*) and *Paulownia elongata* are both rapidly growing hardwoods that have shown promise as feedstocks for biochar that can be used as fillers in common rubber composites such as Hevea natural rubber, styrene-butadiene, and polybutadiene. In this work, poplar and paulownia biochars were used to partially replace carbon black as filler in guayule rubber composites. Guayule composites with up to 60% of the carbon black replaced with poplar or paulownia biochar had higher tensile strength, elongation, and toughness compared to the 100% carbon black-filled control. These composites would be excellent candidates for rubber applications such as gloves, belts, hoses, and seals, while reducing dependence on fossil fuels and Hevea natural rubber.

Keywords: guayule rubber; biochar; poplar; paulownia; rubber composite

check for updates

Citation: Peterson, S.C.; McMahan, C.M. Replacement of Carbon Black with Coppiced Biochar in Guayule Rubber Composites Improves Tensile Properties. *J. Compos. Sci.* **2023**, *7*, 499. https://doi.org/10.3390/jcs7120499

Academic Editors: Francesco Tornabene and Traian Dumitrica

Received: 27 September 2023
Revised: 10 November 2023
Accepted: 28 November 2023
Published: 2 December 2023

1. Introduction

The guayule shrub is a promising industrial crop since it produces natural rubber (NR) and grows well in arid lands that may not compete with food production [1,2]. Currently, Southeast Asia produces the most natural rubber, accounting for over 90% of the world supply [1]. Southeast Asian natural rubber is sourced from *Hevea brasiliensis*, commonly known as the rubber tree. Natural rubber is a critical resource for the U.S. automotive industry, national security, transportation, and medical products. Providing a domestic, alternative source of NR would reduce US dependence on imported NR. Besides these fundamental areas, other value-added applications of guayule such as biofuels, chemicals [3], and novel packing materials [4] are being studied. A significant advantage of guayule NR compared to Hevea NR is that latex products made from guayule do not contain the proteins that cause Type I latex allergies [5]. Guayule latex substitutes for many common latex items made from Hevea have been successfully made [6].

Biochar is a sustainable form of carbon from the pyrolysis (heat treatment in the absence of oxygen) of biomass [7]. Most biochar research traditionally has been focused on carbon sequestration [8–10], but applications of this versatile material also include catalysts [11–13], filtration media [14,15], and sorptive media [16–18]. Since biochar is renewable, it has also been studied as a potential replacement for carbon black (CB) filler, which is sourced from fossil fuels. Dependence on fossil fuels can be problematic since global oil prices are volatile due to political conflicts [19,20]. Reducing dependence on fossil fuels and increasing sustainable options also reduces pollution [21]. However, replacing

CB with biochar has its challenges, one of the most significant being carbon content. CB production has been established for decades, and it is routine to achieve >99% carbon content. Biochar's versatility in feedstocks (any carbon-containing biomass) is also its greatest weakness when it comes to carbon purity, because the pyrolysis process (heat treatment in the absence of oxygen) necessary to make solid biochar also creates gaseous (syngas), liquid (bio-oil) and ash coproducts. However, biochar with higher carbon purity (>85%) can be created if one is careful in choosing the correct feedstocks and pyrolysis processing parameters. Past work in our lab has shown that hardwoods have been better suited for high carbon content biochar production [22] compared to other biomass feedstocks such as grasses, crop stovers, or other agricultural residues [23,24]. Coppiced hardwoods, which are cut, regrown, and then recut periodically from the same stump, have the added advantage of higher biomass yields per area. *Paulownia elongata* is a coppiced hardwood that has a rapid growth rate [25,26] and can be easily grown over a large area of the Southeastern United States [27]. Another excellent feedstock candidate for high carbon-content biochar is hybrid poplar [28,29]. Genetic studies of poplar have led to clones that can be tailored for better drought resistance, pest resistance, and higher biomass yields [30,31], and its preferred hardiness zones stretch nearly across the entirety of the United States and Canada.

Previous studies have been performed using torrefied biomass to replace CB in guayule rubber [32]. Torrefaction is a milder form of pyrolysis that typically only reaches a maximum temperature of 200–300 °C, while most biochar is pyrolyzed at temperatures ranging from 500 to 1000 °C. In that work, replacing CB with torrefied biomass (from almond shells and rice hulls) decreased tensile strength and modulus in the composite while increasing elongation, suggesting a weaker filler network in the rubber matrix.

Research on alternative fillers for guayule rubber such as fly ash [33], eggshell [34,35], and other waste-derived materials [36,37] has also been studied in detail by Cornish and coworkers. Their results with micro-sized eggshell [36] suggest that a synergistic reinforcing effect of CB with a network formed by the guayule rubber and waste-derived materials does not occur with Hevea natural rubber, giving guayule rubber composites a unique compatibility with CB-blended fillers. In this work, we evaluated the viability of coppiced-wood biochars, specifically poplar and paulownia, as full or partial replacements for CB in guayule rubber composites. By maximizing the ratio of biochar to CB, these composites can be made more sustainable and reduce both our dependence on fossil fuels and imported Hevea natural rubber.

2. Materials and Methods

2.1. Materials Used

Guayule latex was generously provided by the Yulex Corporation (San Diego, AZ, USA), from commercial production of guayule shrubs in Arizona. Shrubs were harvested and chipped, and the latex was extracted and concentrated using an aqueous process [38]. The latex was air dried to a solid prior to compounding. Biochar samples made from poplar (*Populus tremuloides*) and Paulownia (*Paulownia elongata*) hardwoods were supplied by Green Carbon Nanostructures Corporation (Hartland, WI, USA). Carbon black was N-339 grade (Vulcan M) provided by the Cabot Corporation (Alpharetta, GA, USA). Toluene from Fisher (Waltham, MA, USA) was ACS grade and used as provided.

2.2. Chemical and Physical Material Properties

Elemental analysis of carbon, hydrogen, and nitrogen, and densities of the samples were all measured as detailed in a previous manuscript [39]. Molecular weight information on the guayule natural rubber used was measured using gel permeation chromatography. Approximately 3 mg of rubber was solubilized in 3 mL of tetrahydrofuran (THF) via gentle shaking overnight. The solution was filtered through a 1.6 µm glass microfiber GF/A filter and injected into an Agilent 1100 series HPLC (Agilent Technologies, Palo Alto, CA, USA) (1 mL/min, 35 °C, 100 µL injection volume, THF continuous phase) with a refractive index detector (RI) (Agilent 1260 Infinity, dn/dc = 0.129), a UV detector (Agilent 1100 series

@254 nm), and a multi-angle laser light-scattering (MALLS) detector (DAWN Heleos II, Wyatt Technology, Santa Barbara, CA, USA). The system was equipped with two Agilent PLgel 10 µm Mixed-B 300 × 7.5 mm columns in series. Chromatograms were collected and the molecular weight calculated using ASTRA V6 software (Wyatt Technology, Santa Barbara, CA, USA).

Scanning electron microscopy (SEM) images were obtained using a JEOL JSM-6010A (JEOL Inc., Peabody, MA, USA). CB, biochar, or the fractured surfaces of rubber composite samples pulled during tensile testing were mounted on SEM stubs and sputter coated with gold using an SPI sputter coater (Structure Probe Inc., West Chester, PA, USA).

2.3. Thermal Stability

Thermogravimetric analysis (TGA) was carried out using a TA Instruments Q500 TGA (New Castle, DE, USA). A small amount of solid sample (10–15 mg) was weighed into a platinum pan, then underwent a heating rate of 10 °C/min in air, from room temperature to 1000 °C.

2.4. Biochar Milling

Poplar and paulownia biochars were milled in an SFM-1 planetary ball mill (model QM-3SP2, MTI Corporation, Richmond, CA, USA) using stainless steel milling jars (500 mL) and lids. Yttrium-stabilized zirconia spheres (3 mm diameter, Inframat Corporation, Manchester, CT, USA) were used as the milling media. The planetary ball mill was set to accelerate to 500 rpm and programmed to run for 30 min in one direction, slowed down to zero rpm with a 6 min rest, then accelerated to 500 rpm in the opposite direction for 30 min.

2.5. Formation of Rubber Composites and Tensile Testing

Rubber composites were solid phase mixed using a 75 mL C.W. Brabender Intelli-Torque Plasti-Corder torque rheometer. The recommended fill factor of 75% was used. Guayule rubber was masticated at 60 rpm and 120 °C. Then, 2,2,4-trimethyl-1,2-dihydroquinone, *N*-1,3-dimethylbutyl-*N*-phenyl-p-phenylene diamine, zinc oxide, the appropriate amount of filler (see Table 1 below), and stearic acid were added. At this point, a 5 kg weight was placed on top of the piston and mixing continued at 120 °C for an additional 10 min. After removing the solid composite from the chamber, it was rolled and sheeted by an MTI HR01 hot rolling machine (Richmond, CA, USA), with the rollers set to 25 °C and a nip width of 2 mm. The Brabender was then adjusted to 100 °C, and the sheeted mixture was added back into the mixer with sulfur and N-cyclohexyl-2-benzothiazolesulfenamide and allowed to mix for an additional 3 min.

All rubber composites were 30% by weight (42.85 parts per hundred (phr)) total filler. The following masterbatch components were identical for all samples tested: guayule rubber, 100 phr; 2,2,4-trimethyl-1,2-dihydroquinone, 1 phr; *N*-1,3-dimethylbutyl-*N*-phenyl-p-phenylene diamine, 0.5 phr; stearic acid, 2 phr; zinc oxide, 5 phr; sulfur, 2 phr; *N*-cyclohexyl-2-benzothiazolesulfenamide, 1 phr. Filler composition was varied and is specified in Table 1 below.

Rubber composites were loaded into a 102 mm × 102 mm × 2 mm window-type mold and cured in a Carver press preheated to 160 °C, where they were compressed at 89 kN for 10 min to form cured sheets. Tensile properties were measured using an Instron 55R1123C5420 (Instron, Inc., Norwood, MA, USA) using Bluehill software version 3.61. At least four replicates of each rubber composite sample were tested.

Table 1. Filler composition for guayule rubber samples (phr).

Filler Composition	CB	Poplar Biochar	Paulownia Biochar
100% CB (control)	42.85	0	0
100% poplar	0	42.85	0
100% paulownia	0	0	42.85
70:30 CB to poplar	30	12.85	0
60:40 CB to poplar	25.71	17.14	0
50:50 CB to poplar	21.43	21.43	0
40:60 CB to poplar	17.14	25.71	0
30:70 CB to poplar	12.85	30	0
20:80 CB to poplar	8.57	34.28	0
70:30 CB to paulownia	30	0	12.85
60:40 CB to paulownia	25.71	0	17.14
50:50 CB to paulownia	21.43	0	21.43
40:60 CB to paulownia	17.14	0	25.71
30:70 CB to paulownia	12.85	0	30
20:80 CB to paulownia	8.57	0	34.28

2.6. Solvent Swelling Experiments

Cross-link densities of the rubber composites were determined using solvent swelling methods, based on ASTM D3616-95 [40]. Three samples of each composite were cut from cured sheets to dimensions of 6.35 mm wide by 1.8–2.0 mm thick by 25 mm long, and the sample mass was measured. Samples were placed in beakers containing 80 mL of toluene and left covered for one week to equilibrate. Samples were then removed, blotted dry, and re-weighed. The swelling ratio of the samples was calculated as follows:

$$Swelling\ ratio\ (\%) = \frac{\left(W_f - W_0\right)}{W_0} * 100$$

where W_0 and W_f are the weights of the sample initially and after equilibrium, respectively. The swelling ratio of each sample was the average of three specimens. Crosslink densities of the samples were calculated using the Flory–Rehner equation [41]:

$$\rho_c = -\frac{1}{2V_s}\frac{\ln\left(1 - v_r\right) + v_r + \chi v_r^2}{{v_r}^{1/3} - v_r/2}$$

where ρ_c is the crosslink density in mol/cm^3, v_r is the volume fraction of swollen vulcanized rubber at equilibrium, V_s is the mole volume of solvent at room temperature in cm^3/mol (106.9 for toluene), and χ is the Flory–Huggins polymer–solvent interaction parameter (0.393) [37]. Since these samples contained CB and/or biochar as filler, the following equation was used to take the filler effect into consideration [42]:

$$\frac{v_r}{v_{rf}} = 1 - \left\{3c\left[1 - v_r^{1/3}\right] + v_r - 1\right\}\frac{\phi}{1 - \phi}$$

where v_{rf} is the volume fraction of swollen filled rubber, c is the rubber interaction parameter (1.17 for natural rubber [43]), and ϕ is the volume fraction of filler in the unswollen filled rubber. Solving this equation for v_r was used in the Flory–Rehner equation to calculate ρ_c, crosslink density.

3. Results and Discussion

3.1. Chemical and Physical Properties

Elemental composition, ash content, and densities of the poplar and paulownia biochars relative to CB are shown in Table 2 below. These particular biochar samples were chosen because of their high carbon content and low ash content. The densities are similar to CB as well.

Table 2. Physical and elemental properties of CB, poplar and paulownia biochars.

Sample	C (%)	H (%)	N (%)	O (%) [a]	Ash (%)	Density (g/cm^3)
CB [b]	>99	<1	<1	<1	<1	1.7–1.9
poplar	87.2 ± 0.5	1.8 ± 0.2	0.12 ± 0.04	6.5	4.3	1.68
paulownia	95.2 ± 0.7	1.4 ± 0.3	0.02 [c]	0.9	2.5	1.76

[a] oxygen content calculated by difference; [b] data supplied by the manufacturer; [c] standard error was negligible.

SEM images showing the morphology of poplar and paulownia biochars compared to CB can be seen in Figure 1. Both CB and poplar have similar aggregate structures, while the original woody structure of paulownia is more evident compared to poplar.

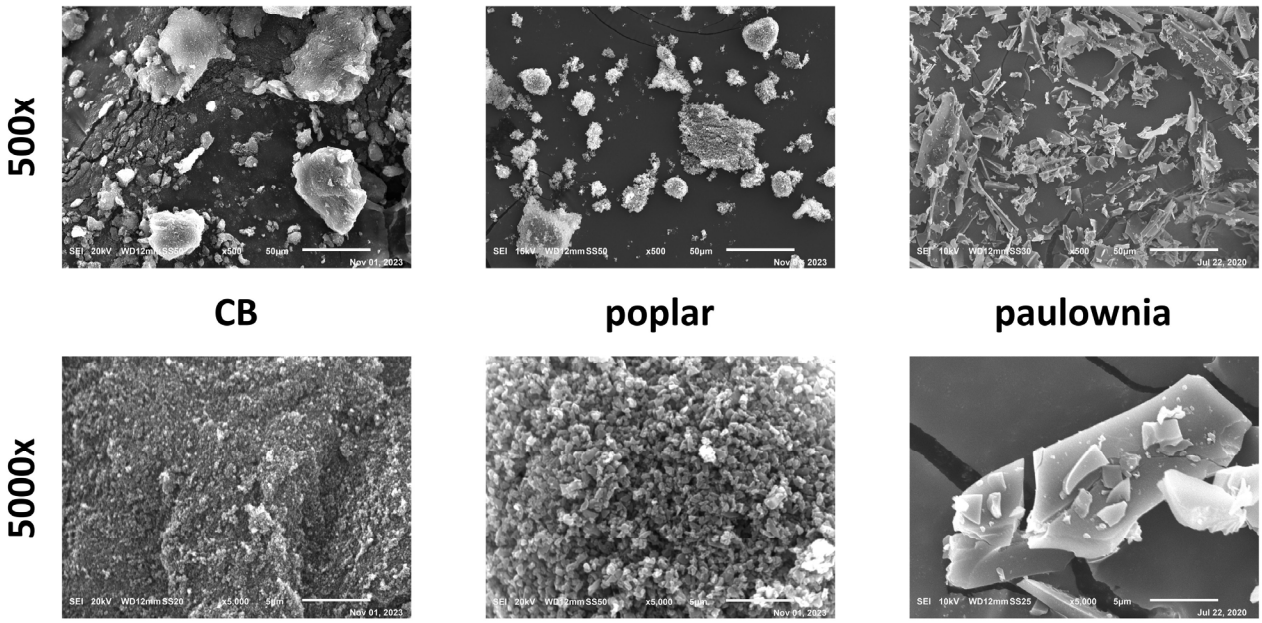

Figure 1. SEM images of CB, poplar biochar, and paulownia biochar at 500× (**top** row) and 5000× (**bottom** row). For images at 500×, the white scale bar in the lower right corner represents 50 microns, and for images at 5000×, it represents 5 microns.

The guayule NR used was found to have an M_w value of 1.80 ± 0.03 MDa with a polydispersity of 1.86, and an M_p value of 1.56 ± 0.01 MDa with a polydispersity of 1.00. TGA analysis results for guayule rubber in air can be seen in Figure 2. It should be noted that the guayule rubber sample as received was partially coagulated, so it was a very heterogeneous mixture of liquid latex and congealed solid rubber. All the samples and resulting data shown in this study were obtained from composites made from the largest piece of congealed rubber. At approximately 100 °C, water loss is evident. Guayule has typical natural rubber derivative T_{max} values of 360 °C and 490 °C, and the small derivative peak at roughly 420 °C is most likely due to residual plant tissues [44].

3.2. Crosslinking and Tensile Properties

Mechanical properties of NR are greatly influenced by the chemical crosslinking that occurs during curing, as crosslinking prevents the NR polymeric chains from sliding and becoming entangled under load stresses [45]. Crosslink densities for the samples are shown in Table 3.

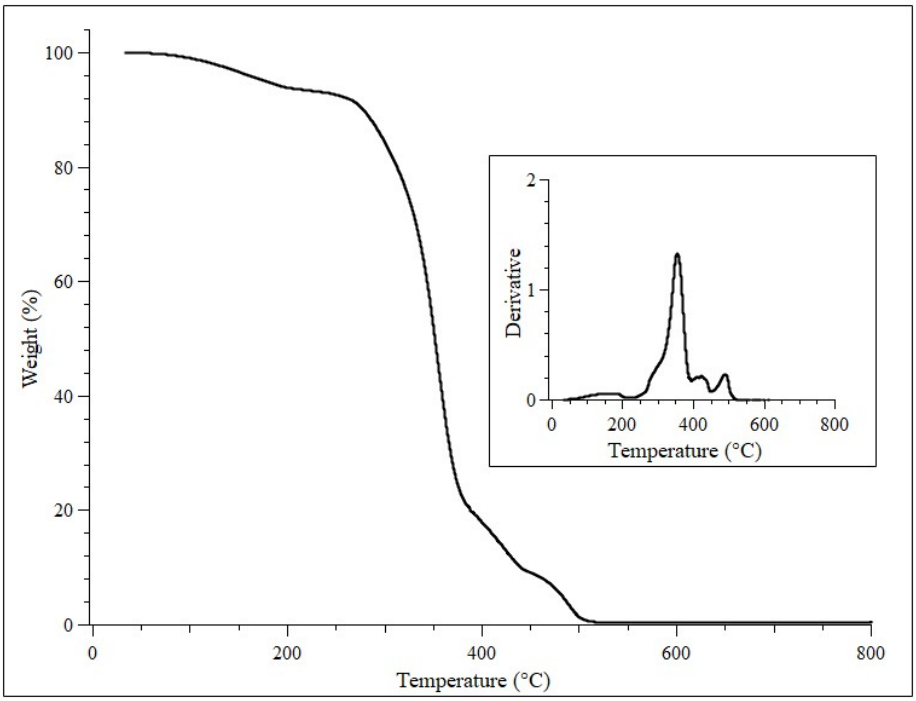

Figure 2. TGA results for weight loss of guayule as a function of temperature. Inset plot is the derivative curve.

Table 3. Swelling ratio and crosslink density values for poplar/CB and paulownia/CB rubber composites.

Sample/Filler Composition	Swelling Ratio at Equilibrium (%)	Crosslink Density (10^{-3} mol/cm^3)
100% CB control	152	0.30
30/70 poplar/CB	169	0.26
40/60 poplar/CB	175	0.25
50/50 poplar/CB	188	0.22
60/40 poplar/CB	231	0.16
70/30 poplar/CB	246	0.15
80/20 poplar/CB	272	0.13
100% poplar	303	0.11
30/70 paulownia/CB	150	0.33
40/60 paulownia/CB	170	0.26
50/50 paulownia/CB	176	0.25
60/40 paulownia/CB	206	0.20
70/30 paulownia/CB	234	0.16
80/20 paulownia/CB	221	0.18
100% paulownia	243	0.15

Figure 3 shows the tensile properties of the CB control and all the rubber composites. All these samples have a total filler concentration of 30%, and the ratio of CB to either poplar or paulownia biochar was varied. The 100% CB-filled sample (the leftmost bar) serves as the control to which all other samples are compared (dotted line). The crosslink density trends of the composites correlated with tensile strength; as the filler ratio of biochar to CB increased, the crosslink density decreased.

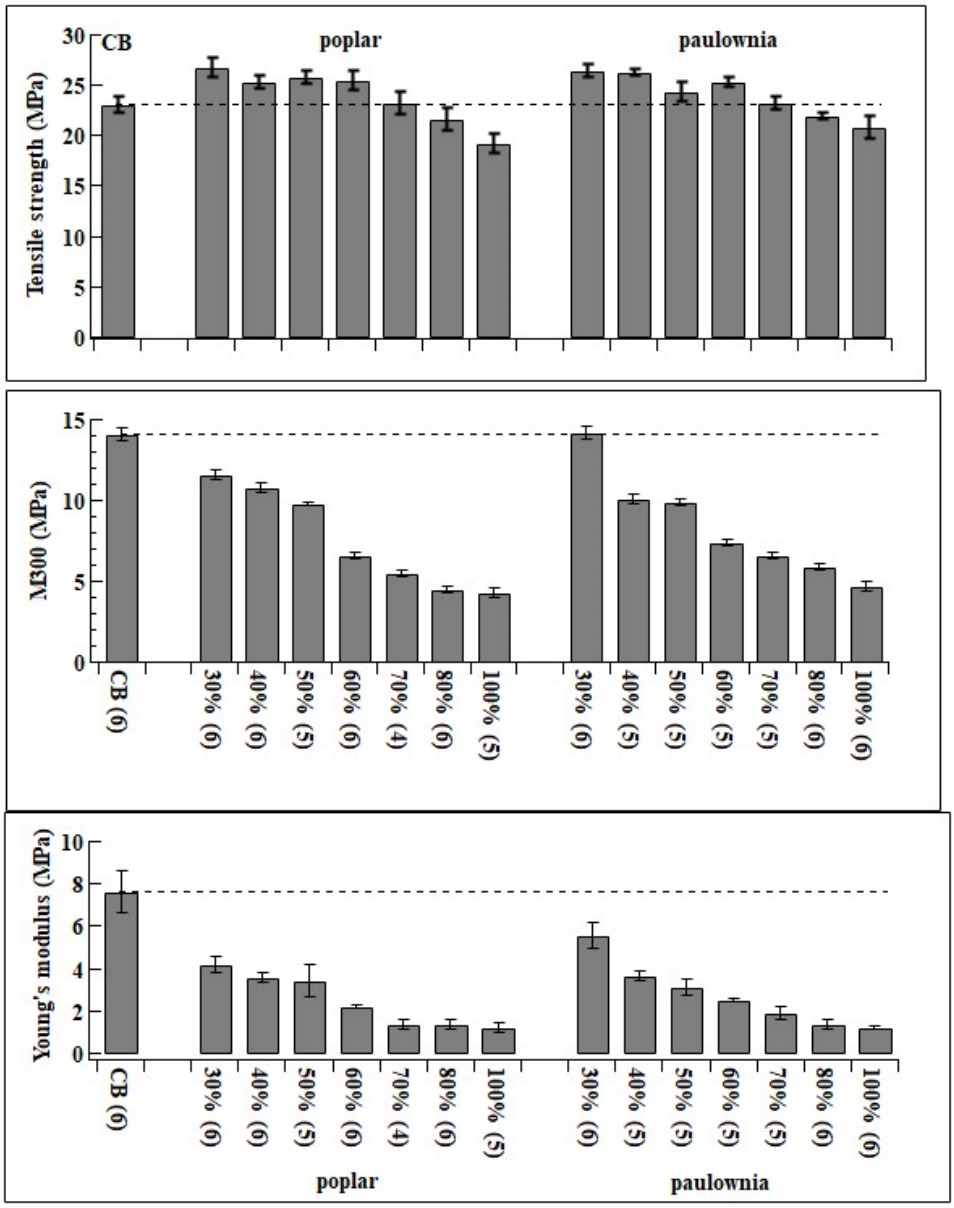

Figure 3. Tensile strength, modulus at 300% elongation, and Young's modulus of guayule rubber composite samples. CB = carbon black. Percentages at the bottom of the plot represent the percentage of CB replaced by either poplar or paulownia biochar, followed by the number of replicates in parenthesis.

As seen from Figure 3, incorporation of coppiced biochars resulted in rubber composites with equal or higher tensile strength compared to carbon black-filled composites at up to 70% replacement using either poplar or paulownia biochar. Modulus values (Young's and 300% Modulus) were lower in all cases and decreased systematically as CB was replaced with the biochar fillers. As seen in Figure 4, in all cases, composite elongation was significantly higher when CB was replaced by biochars. Toughness was also higher (Figure 4) for biochar-filled composites at most levels. Overall, the coppiced biochar-filled composites were softer and more extensible than the CB-filled controls, yet had quite high tensile strength. Figure 5 illustrates this with stress–strain curves for several different poplar biochar to CB filler ratios and their accompanying SEM images that show the fractured composite surface after tensile testing. Typically, composites that have better tensile strength will show more homogeneous dispersion of the filler. SEM images (A) and (B) appear very similar with effective dispersion of the filler throughout the rubber matrix.

As the ratio of poplar biochar to CB is increased from image B to C to D, more biochar agglomeration is evident, and the larger size of these agglomerates causes fracture points in the composite, reducing the tensile strength, as seen in Figure 3.

Overall, the biggest sacrifice concomitant with using poplar or paulownia biochar as blended filler in guayule rubber appears as reduced composite stiffness, reflected in the lower M300 and Young's modulus values and shallower slope on the stress–strain curves relative to the CB control (Figure 5). Stiffness of the composites seems to be directly proportional to the amount of CB in the sample. Mechanical property trends found here were similar to those found when CB was substituted with torrefied biomass (from rice hulls and almond shells) [32] or carbon fly ash [33] in guayule rubber composites [32], i.e., modulus was lower and elongation higher as CB levels decreased. However, both studies generally found lower tensile strength with carbon black substitution, while for biochar-filled composites, tensile strength was increased (vs. controls), possibly due to the higher carbon content in biochar fillers, with better compatibility to the NR matrix.

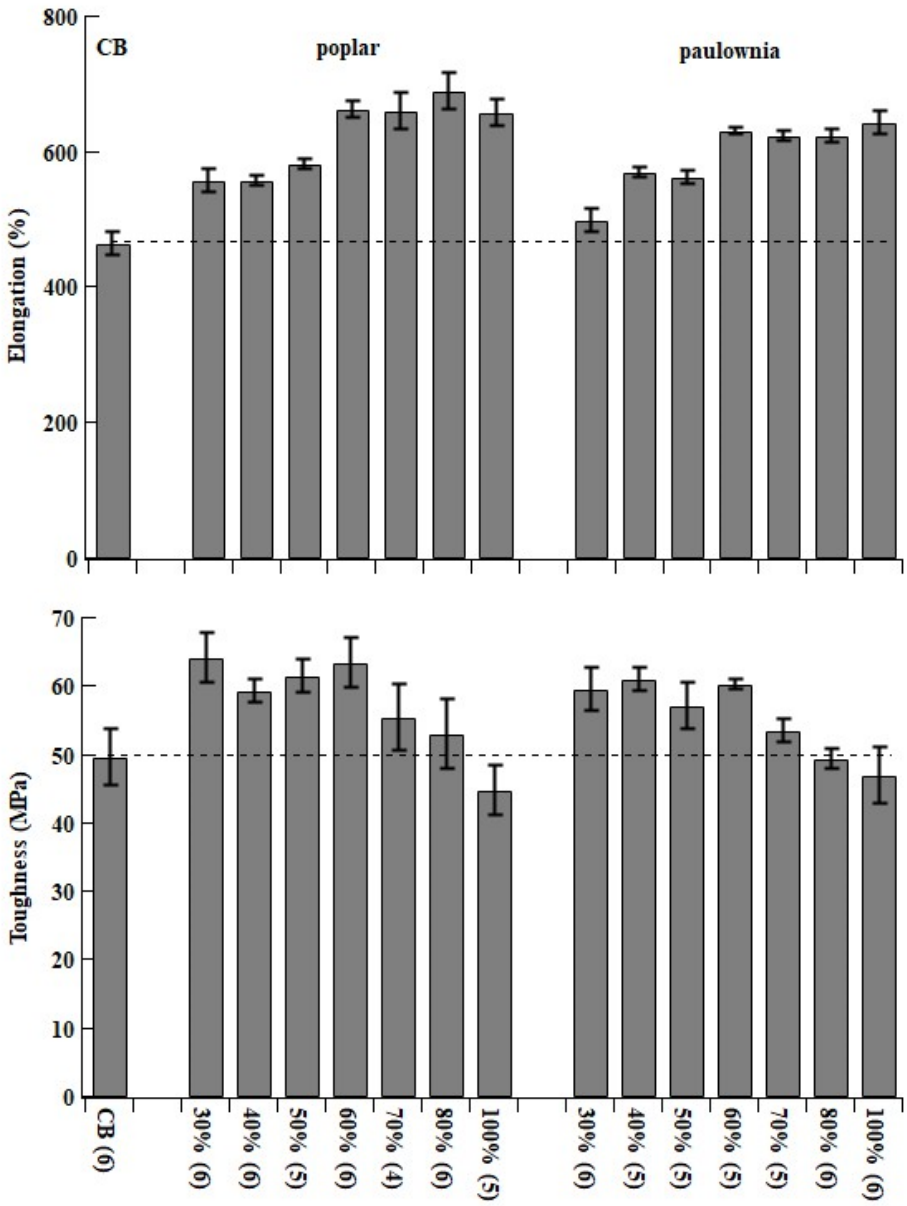

Figure 4. Elongation and toughness of guayule rubber composite samples. CB = carbon black. Percentages at the bottom of the plot represent the percentage of CB replaced by either poplar or paulownia biochar followed by the number of replicates in parenthesis.

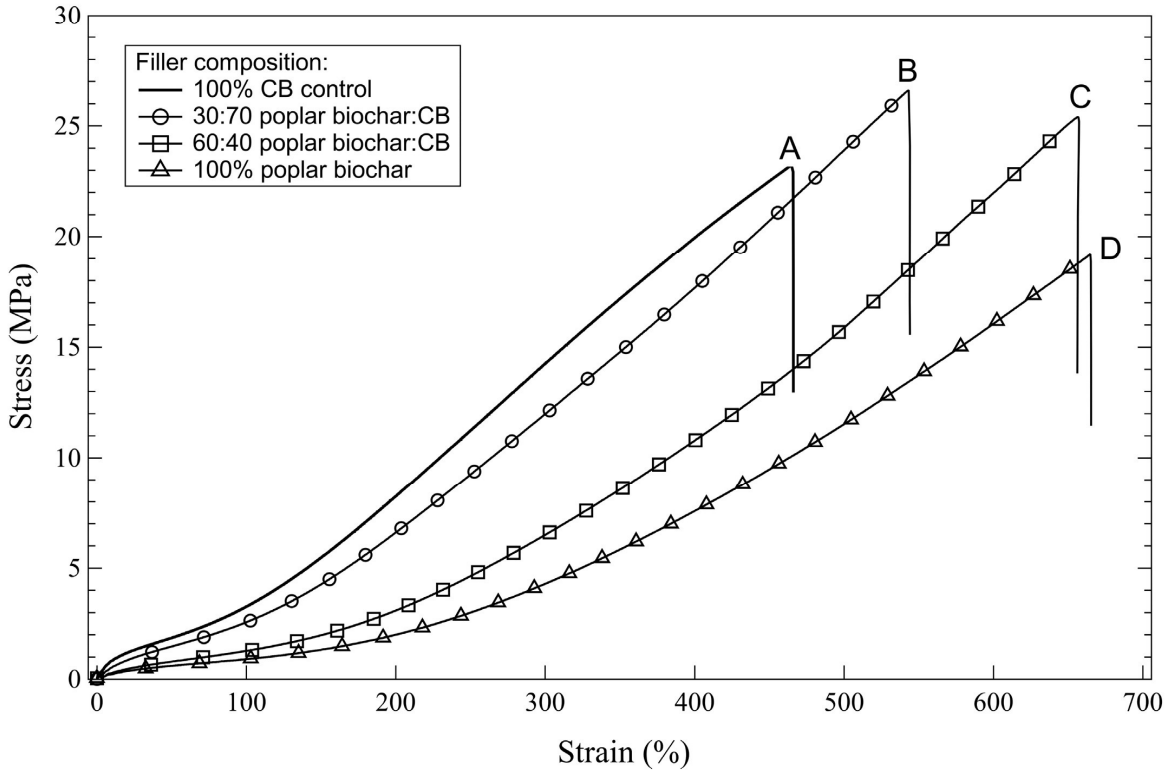

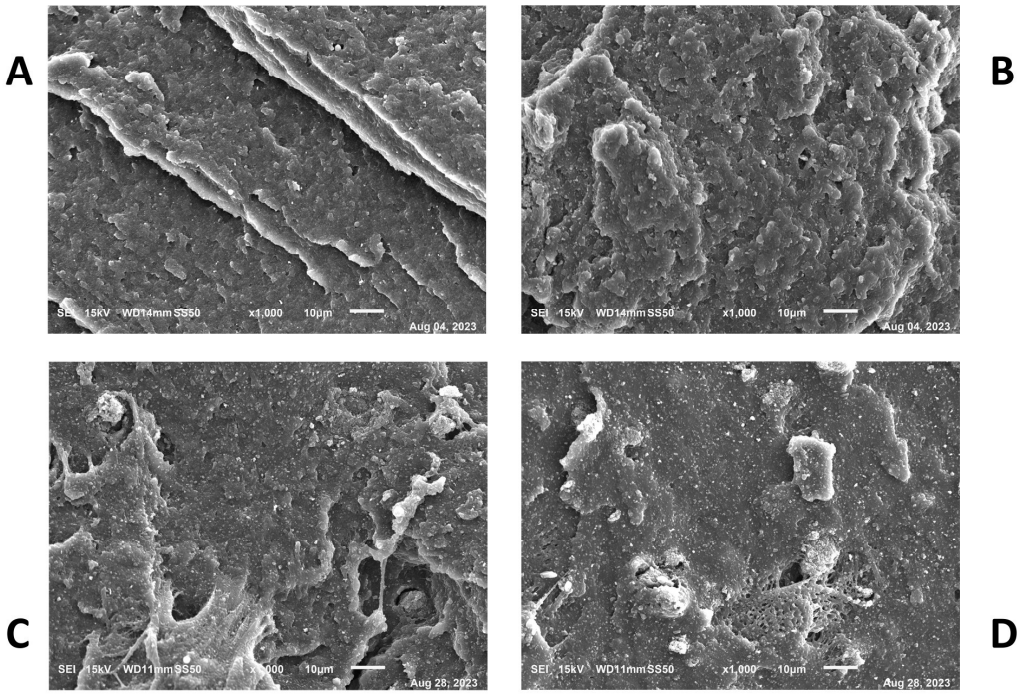

Figure 5. Tensile properties for (**A**) 100% CB-filled control, (**B**) 30:70 poplar biochar to CB filler, (**C**) 60:40 poplar biochar to CB filler, and (**D**) 100% poplar biochar-filled guayule rubber composites. Below the plot are four corresponding SEM images of the fractured surfaces of these same composites at 1000×.

Biochar/CB guayule composites are softer than the CB-filled control, but their superior tensile strength, elongation, and toughness suggest they can be used for rubber applications

such as gloves, belts, hoses, gaskets, and seals. Coppiced biochars and guayule rubber are both sustainable, domestic resources that can be used to reduce dependence on imported natural rubber and fossil fuels.

Author Contributions: Conceptualization, S.C.P.; formal analysis, S.C.P. and C.M.M.; investigation, S.C.P. and C.M.M.; resources, S.C.P. and C.M.M.; writing—original draft, S.C.P.; writing—review and editing, S.C.P. and C.M.M. All authors have read and agreed to the published version of the manuscript.

Funding: USDA, Agricultural Research Service: 5010-44000-187-000-D.

Data Availability Statement: The data presented in this study are openly available in FigShare at 10.6084/m9.figshare.24712434 (Accessed on 1 September 2023).

Acknowledgments: The authors would like to thank Chen Dong for performing GPC experiments; Kelly Utt for SEM imaging; Jason Adkins for performing TGA experiments; and A.J. Thomas for formulating the rubber composite samples and tensile testing, swelling experiments, CHNO, density, and ash measurements. Mention of trade names or commercial products in this publication is solely for the purpose of providing specific information and does not imply recommendation or endorsement by the U.S. Department of Agriculture. USDA is an equal opportunity provider and employer.

Conflicts of Interest: The authors declare no conflict of interest.

References

1. Rasutis, D.; Soratana, K.; McMahan, C.; Landis, A.E. A sustainability review of domestic rubber from the guayule plant. *Ind. Crops Prod.* **2015**, *70*, 383–394. [CrossRef]
2. Foster, K.E.; Karpiscak, M.M.; Taylor, J.G.; Wright, N. Guayule, jojoba, buffalo gourd and Russian thistle: Plant characteristics, products and commercialization potential. *Desert Plants* **1983**, *5*, 112–126.
3. Cheng, F.; Dehghanizadeh, M.; Audu, M.A.; Jarvis, J.M.; Holguin, F.O.; Brewer, C.E. Characterization and evaluation of guayule processing residues as potential feedstock for biofuel and chemical production. *Ind. Crops Prod.* **2020**, *150*, 112311. [CrossRef]
4. César, E.; Castillo-Campohermoso, M.A.; Ledezma-Pérez, A.S.; Villarreal-Cárdenas, L.A.; Montoya, L.; Bandala, V.M.; Rodríguez-Hernández, A.M. Guayule bagasse to make mycelium composites: An alternative to enhance the profitability of a sustainable guayule crop. *Biocatal. Agric. Biotechnol.* **2023**, *47*, 102602. [CrossRef]
5. Cornish, K.; Lytle, C.D. Viral impermeability of hypoallergenic, low protein, guayule latex films. *J. Biomed. Mater. Res.* **1999**, *47*, 434–437. [CrossRef]
6. Cornish, K.; Williams, J.; Hall, J.L.; McCoy, R.G., III. Production and properties of yulex—The natural solution to latex allergy. *Rubber Chem. Technol.* **2008**, *81*, 709–722. [CrossRef]
7. Liu, W.-J.; Jiang, H.; Yu, H.-Q. Development of Biochar-Based Functional Materials: Toward a Sustainable Platform Carbon Material. *Chem. Rev.* **2015**, *115*, 12251–12285. [CrossRef]
8. Ding, X.; Li, G.; Zhao, X.; Lin, Q.; Wang, X. Biochar application significantly increases soil organic carbon under conservation tillage: An 11-year field experiment. *Biochar* **2023**, *5*, 28. [CrossRef]
9. Khoshraftar, Z.; Masoumi, H.; Ghaemi, A. Characterization and evaluation of low-cost biomass-based-AC for CO_2 capture: A review. *Case Stud. Chem. Environ. Eng.* **2023**, *8*, 100373. [CrossRef]
10. Liu, Q.; Meki, K.; Zheng, H.; Yuan, Y.; Shao, M.; Luo, X.; Li, X.; Jiang, Z.; Li, F.; Xing, B. Biochar application in remediating salt-affected soil to achieve carbon neutrality and abate climate change. *Biochar* **2023**, *5*, 45. [CrossRef]
11. Jiang, M.; He, L.; Niazi, N.K.; Wang, H.; Gustave, W.; Vithanage, M.; Geng, K.; Shang, H.; Zhang, X.; Wang, Z. Nanobiochar for the remediation of contaminated soil and water: Challenges and opportunities. *Biochar* **2023**, *5*, 2. [CrossRef]
12. Miao, X.; Chen, X.; Wu, W.; Lin, D.; Yang, K. Topological defects strengthened nonradical oxidation performance of biochar catalyzed peroxydisulfate system. *Biochar* **2023**, *5*, 40. [CrossRef]
13. Wang, C.; Xie, Q.; Dou, X.; Zhang, L.; Yang, X. Conversion of carbonaceous materials into solid acids for tylosin mitigation: Effect of preprocessing methods on the reactivity of sulfonation reaction. *Biochar* **2023**, *5*, 32. [CrossRef]
14. Xiang, W.; Zhang, X.; Chen, J.; Zou, W.; He, F.; Hu, X.; Tsang, D.C.W.; Ok, Y.S.; Gao, B. Biochar technology in wastewater treatment: A critical review. *Chemosphere* **2020**, *252*, 126539. [CrossRef] [PubMed]
15. Palansooriya, K.N.; Yang, Y.; Tsang, Y.F.; Sarkar, B.; Hou, D.; Cao, X.; Meers, E.; Rinklebe, J.; Kim, K.-H.; Ok, Y.S. Occurrence of contaminants in drinking water sources and the potential of biochar for water quality improvement: A review. *Crit. Rev. Environ. Sci. Tec.* **2020**, *50*, 549–611. [CrossRef]
16. Gwenzi, W.; Chaukura, N.; Wenga, T.; Mtisi, M. Biochars as media for air pollution control systems: Contaminant removal, applications and future research directions. *Sci. Total Environ.* **2021**, *753*, 142249. [CrossRef] [PubMed]

17. Peiris, C.; Nawalage, S.; Wewalwela, J.J.; Gunatilake, S.R.; Vithanage, M. Biochar based sorptive remediation of steroidal estrogen contaminated aqueous systems: A critical review. *Environ. Res.* **2020**, *191*, 110183. [CrossRef]
18. Ghosh, D.; Maiti, S.K. Can biochar reclaim coal mine spoil? *J. Environ. Manag.* **2020**, *272*, 111097. [CrossRef]
19. Lee, C.-C.; Olasehinde-Williams, G.; Akadiri, S.S. Are geopolitical threats powerful enough to predict global oil price volatility? *Environ. Sci. Pollut. Res.* **2021**, *28*, 28720–28731. [CrossRef]
20. Rommen, R. Russia and Ukraine are Battling It Out over Gas and Oil Platforms in the Black Sea, UK Ministry of Defence Says. Available online: https://www.businessinsider.com/russia-ukraine-war-battle-gas-oil-platforms-uk-military-intelligence-2023-8 (accessed on 29 August 2023).
21. Bertrand, S. Climate, Environmental, and Health Impacts of Fossil Fuels. Available online: https://www.eesi.org/files/FactSheet_Fossil_Fuel_Externalities_2021.pdf (accessed on 29 August 2023).
22. Peterson, S.C. Coppiced Biochars as Partial Replacement of Carbon Black Filler in Polybutadiene/Natural Rubber Composites. *J. Compos. Sci.* **2020**, *4*, 147. [CrossRef]
23. Mukome, F.N.D.; Zhang, X.; Silva, L.C.R.; Six, J.; Parikh, S.J. Use of Chemical and Physical Characteristics to Investigate Trends in Biochar Feedstocks. *J. Agric. Food Chem.* **2013**, *61*, 2196–2204. [CrossRef]
24. Demirbas, A. Effects of temperature and particle size on bio-char yield from pyrolysis of agricultural residues. *J. Anal. Appl. Pyrol.* **2004**, *72*, 243–248. [CrossRef]
25. Jiménez, L.; Rodríguez, A.; Ferrer, J.L.; Ṕerez, A.; Angulo, V. Paulownia, a fast-growing plant, as a raw material for paper manufacturing. *Afinidad* **2005**, *62*, 100–105.
26. Basu, C.; Joshee, N.; Gezalian, T.; Vaidya, B.N.; Satidkit, A.; Hemmati, H.; Perry, Z.D. Cross-species PCR and field studies on Paulownia elongata: A potential bioenergy crop. *Bioethanol* **2016**, *2*, 12–23. [CrossRef]
27. Institute, W.P. Paulownia Growing Zones. Available online: http://worldpaulownia.com/growing-zones (accessed on 5 September 2023).
28. Zamora, D.S.; Wyatt, G.J.; Apostol, K.G.; Tschirner, U. Biomass yield, energy values, and chemical composition of hybrid poplars in short rotation woody crop production and native perennial grasses in Minnesota, USA. *Biomass Bioenergy* **2013**, *49*, 222–230. [CrossRef]
29. Stanton, B.J.; Haiby, K.; Gantz, C.; Espinoza, J.; Shuren, R.A. The economics of rapid multiplication of hybrid poplar biomass varieties. *Forests* **2019**, *10*, 446. [CrossRef]
30. Tuskan, G.A.; Di Fazio, S.; Jansson, S.; Bohlmann, J.; Grigoriev, I.; Hellsten, U.; Putnam, N.; Ralph, S.; Rombauts, S.; Salamov, A.; et al. The genome of black cottonwood, *Populus trichocarpa* (Torr. & Gray). *Science* **2006**, *313*, 1596–1604. [CrossRef] [PubMed]
31. Zalesny, R.S.; Hall, R.B.; Zalesny, J.A.; McMahon, B.G.; Berguson, W.E.; Stanosz, G.R. Biomass and Genotype × Environment Interactions of *Populus* Energy Crops in the Midwestern United States. *Bioenergy Res.* **2009**, *2*, 106–122. [CrossRef]
32. Torres, L.F.; McCaffrey, Z.; Washington, W.; Williams, T.G.; Wood, D.F.; Orts, W.J.; McMahan, C.M. Torrefied agro-industrial residue as filler in natural rubber compounds. *J. Appl. Polym. Sci.* **2021**, *138*, 50684. [CrossRef]
33. Barrera, C.S.; Cornish, K. Novel Mineral and Organic Materials from Agro-Industrial Residues as Fillers for Natural Rubber. *J. Polym. Environ.* **2015**, *23*, 437–448. [CrossRef]
34. Ren, X.; Geng, Y.; Soboyejo, A.B.O.; Cornish, K. Reinforced mechanical properties of functionalized silica and eggshell filled guayule natural rubber composites. *Rubber Chem. Technol.* **2019**, *92*, 687–708. [CrossRef]
35. Ren, X.; Cornish, K. Eggshell improves dynamic properties of durable guayule rubber composites co-reinforced with silanized silica. *Ind. Crops Prod.* **2019**, *138*, 111440. [CrossRef]
36. Barrera, C.S.; Cornish, K. High performance waste-derived filler/carbon black reinforced guayule natural rubber composites. *Ind. Crops Prod.* **2016**, *86*, 132–142. [CrossRef]
37. Barrera, C.S.; Cornish, K. Processing and mechanical properties of natural rubber/waste-derived nano filler composites compared to macro and micro filler composites. *Ind. Crops Prod.* **2017**, *107*, 217–231. [CrossRef]
38. Cornish, K.; McCoy, R.G., III; Martin, J.A.; Williams, J.; Nocera, A.J. Biopolymer Extraction from Plant Materials. U.S. Patent 7923039, 12 April 2011.
39. Peterson, S.C.; Thomas, A.J. Lauric Acid Treatments to Oxidized and Control Biochars and Their Effects on Rubber Composite Tensile Properties. *C* **2022**, *8*, 58. [CrossRef]
40. *ASTM D3616-95(2019)*; Standard Test Method for Rubber-Determination of Gel, Swelling Index, and Dilute Solution Viscosity. ASTM International: West Conshohocken, PA, USA, 2019. [CrossRef]
41. Flory, P.J.; Rehner, J., Jr. Statistical mechanics of cross-linked polymer networks. II. Swelling. *J. Chem. Phys.* **1943**, *11*, 521–526. [CrossRef]
42. Mok, K.L.; Eng, A.H. Characterisation of crosslinks in vulcanised rubbers: From simple to advanced techniques. *Malays. J. Chem.* **2018**, *20*, 118–127.
43. Chaikumpollert, O.; Yamamoto, Y.; Suchiva, K.; Kawahara, S. Mechanical properties and cross-linking structure of cross-linked natural rubber. *Polym. J.* **2012**, *44*, 772–777. [CrossRef]

44. Bhowmick, A.K.; Rampalli, S.; Gallagher, K.; Seeger, R.; McIntyre, D. The degradation of guayule rubber and the effect of resin components on degradation at high temperature. *J. Appl. Polym. Sci.* **1987**, *33*, 1125–1139. [CrossRef]
45. Kim, D.Y.; Park, J.W.; Lee, D.Y.; Seo, K.H. Correlation between the Crosslink Characteristics and Mechanical Properties of Natural Rubber Compound via Accelerators and Reinforcement. *Polymers* **2020**, *12*, 2020. [CrossRef]